Materials under Shock Loading: from Biot's Theory to Nano-Poromechanics

Ahmad K. Al-Qananwah[1], Joel Koplik[2], Yiannis Andreopoulos[3]

[1]Department of Mechanical Engineering, The City College of New York/CUNY, New York, NY 10031, USA. Email: PH: (212) 650-6706; FAX: (212) 650-8013; email: akna911@yahoo.com
[2]Department of Physics, The City College of New York/CUNY, New York, NY 10031, USA. PH: (212) 650-8162; FAX: (212) 650-6835; email: koplik@sci.ccny.cuny.edu
[3]Department of Mechanical Engineering, The City College of New York/CUNY, New York, NY 10031, USA. PH: (212) 650-5206; FAX: (212) 650-8013; email: andre@ccny.cuny.edu

ABSTRACT

Porous materials are known to be effective in mitigating the impact of shock/blast waves. Nano-structured materials appear to have an even greater potential for such mitigation because of their high surface-to-volume ratio, a property which attenuates shock wave propagation substantially. Molecular dynamics was used to explore the effects of this remarkable characteristic on the behavior of traveling shocks impacting on solid materials with and without a porous structure attached. The materials involved were represented by realistic interaction potentials. Cases with various values of porosity have been investigated and the results indicate that the presence of a nano-porous material layer in front of a target wall reduces the energy deposited inside the solid by about 30 percent, while at the same time considerably decreasing its loading rate.

INTRODUCTION

Propagation of nonlinear waves in porous media at the macroscopic level has attracted the attention of many researchers. Of particular interest is the interaction of shock waves with gas-solid mixtures where a substantial amount of experimental, theoretical and computational work has been reported. Modeling these phenomena is based on microscopic conservation laws (mass, momentum, and energy) from which macroscopic evolution equations (ordinary and partial differential equations) are derived, complemented by appropriate closures. A large number of papers have appeared in the literature following Biot's pioneering work (1941), referring to microscopic representations of the phase balance equations within the framework of the theory of mixtures (Levy et al., 1995; Baer & Nunziato, 1986; Bear & Bachmat, 1990). Porous materials have long been known to be effective in blast mitigation strategies (Gubaidullin et al., 2003; Seitz & Skews, 1996; Seitz & Skews, 2003; Mazor et al., 1994, Kazemi-Kamyab et al. 2011; Kitagawa et al. 2006; Britan & Ben-Dor, 2006;). Nano-structured materials appear to have an even greater potential for blast mitigation because of their high surface-to-volume ratio, a geometric factor which substantially attenuates shock wave propagation. In the present work, a molecular dynamics, MD, approach was used to explore the effects of this remarkable property on the behavior of traveling shocks impacting on solid materials.

The shock wave at the continuum level is considered a discontinuity with rather unknown properties inside and its reflection over flat surfaces occurs at the same time with its impact,

since the shock thickness is not resolved. Typically, the process of reflection has a time scale of 0.25 ns for shock thicknesses and propagation velocities of 100 nm and 400 m/s, respectively. These high spatial and temporal resolution requirements of this interaction necessitate the use of atomistic level computer simulations. In the present work nanoscale resolution of the mutual interaction between a shock wave and structured materials is used which includes, for the first time, a simultaneous and integrated/coupled treatment of multiple wave phenomena in both gas and solid phases. The present contribution complements our experimental and computational works with periodic composite structures and functionally graded materials subjected to shock loading (Gong & Andreopoulos, 2008, 2009; Subramaniam et al., 2009; Andreopoulos et al., 2007; Andreopoulos, 2013) at the macroscopic level, and has the potential to bridge the gap between atomistic and meso-scale modeling. Previous work describes shock interactions only at a much coarser level by averaging over atomic variables, and can only address this issue by trial and error.

MOLECULAR DYNAMICS (MD)

In an MD simulation (Allen & Tildesley 1987; Koplik & Banavar, 1995), one integrates Newton's equations for individual atoms, using a specified interaction potential, and then averages over atomic degrees of freedom to obtain the continuum fields relevant to larger scale calculations. For example, local density, velocity and temperature fields are found by dividing the simulation domain into sampling bins and computing the average number, velocity and kinetic energy of the atoms contained in each bin. The computational setup included a moving piston, a gas region and a target solid wall with and without a porous structure attached (see figure 1).

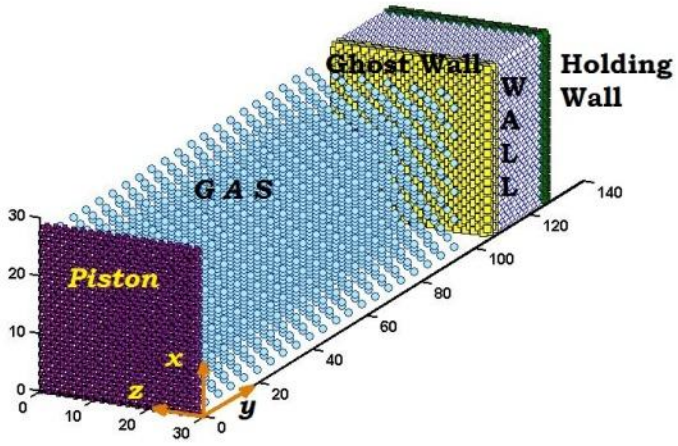

Figure 1: Computational setup

The materials involved were represented by realistic interaction potentials. The gas molecules and the atoms in the piston and holding wall interact via a basic, two-body, Short Range Attractive potential (SHRAT) of Lennard-Jones form (Hess & Kroger, 2002; Stankovic et al., 2004). The SHRAT potential takes the form

$$U^{SHRAT}(r) = \begin{cases} \frac{512}{27}\phi_0 \left(1-\frac{r}{\psi}\right)^3 \left(3-2\frac{r}{\psi}\right)^3, & r \le 1.5\psi \\ 0, & r > 1.5\psi \end{cases} \quad (1)$$

where r is the separation between two atoms, ϕ_0 is the depth of the potential well and ψ controls the cutoff distance and roughly corresponds to the atomic diameter. This potential is similar in shape to a standard Lennard-Jones function. Details of the approach are described in Al-Qananwah et al. (2013).

In MD the stress tensor and heat flux were evaluated by using relations which do not assume or invoke any constitutive law between stress and strain or heat flux and temperature. Shear and bulk moduli were evaluated independently of constitutive relations. The shock wave has been generated by the sudden forward motion of the piston and the bulk flow parameters remained the same as in the previous case where the shock impacted a solid wall.

RESULTS

Figure 2.1 shows an x-t plot of pressure contours in the flow along the gas channel behind the moving shock wave at various instances. The shock impacts the end wall (target) and it is subsequently reflected moving in the opposite direction, towards the piston. At the same time, it is transmitted into the solid phase with energy being exchanged, so that part of the shock wave energy is reflected back into the gas channel and the remaining part is exchanged with the solid molecules. The transmitted shock starts propagating inside the solid structure till it hits the holding wall.

The reflection of the shock over the end wall is associated with a considerable increase in pressure and a pressure ratio of about 10 across the incoming shock wave is been observed; According to the classical shock tube theory, the corresponding pressure ratio in the case of a rigid wall reflection P_5/P_2, is more than 33 for the same pressure ratio across the incoming shock of 10. This comparison clearly demonstrates the striking differences between the present case with an elastic end wall and the classical shock reflection off a rigid body planar surface. In addition, due to the energy exchange with the solid molecules, there is a pressure drop behind the reflected shock as it propagates back into the gas channel.

Figure 2.2 shows the velocity profiles of the shocked gas particles ahead of the piston which is the same as that of the piston. The results show that the distance between the shock front and the piston is getting greater as the simulation time increases since the shock speed is higher than the induced velocity of the molecules behind. Once it hits the target, reflection causes deceleration of the gas flow and eventually the flow changes direction towards the piston. When the shock hits the solid wall, not only energy is exchanged, but also the solid structure deforms, initially pushed and displaced in the downstream direction and subsequently in the opposite direction, which causes the gas flow to change direction. In that respect, the solid phase wall behaves like a vibrating elastic wall which is initially displaced in the y-positive direction during which the flow is decelerated followed by a displacement in the y- negative direction which results in a push of the gas molecules in the same direction. This behavior shows some strong similarities with the corresponding continuum case of shock waves impacting elastics plates which has only recently been studied in Gong & Andreopoulos (2009). In such situations the plate starts to vibrate while at the same time it affects the flow behind the reflected shock wave in a fully coupled manner under a two-way interaction. This strong coupling changes the

dynamics of the plate by reducing the vibrational frequencies due to increased damping in the combined fluid-structure system.

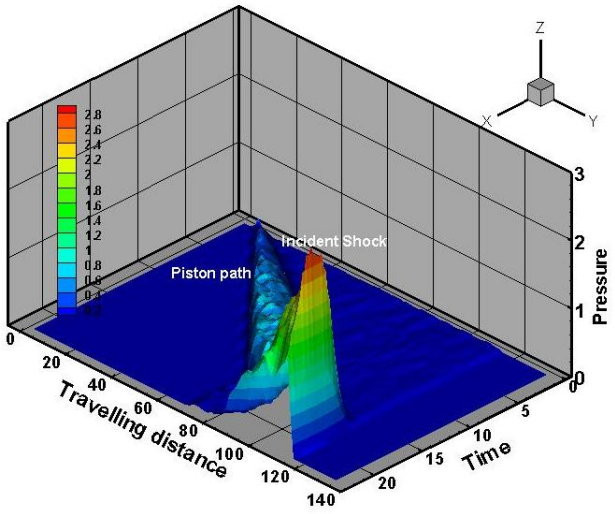

Figure 2.1: Pressure contours in the gas flow domain generated by the propagating shock wave at various times. Length scale ψ_w , time scale $\psi_w(m_w/\phi_{0w})^{1/2}$,pressure scale ϕ_{0w}/ψ_w^3.

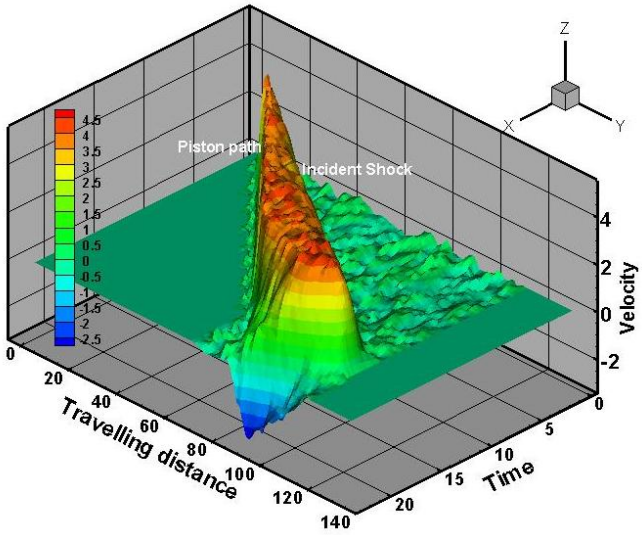

Figure 2.2: Velocity contours in the gas flow domain generated by the propagating shock wave at various times. Length scale ψ_w, time scale $\psi_w(m_w/\phi_{0w})^{1/2}$, velocity scale $\sqrt{\phi_{0w}/m_w}$.

THE POROUS WALL CASE

A porous structure was designed by removing some of the solid particles to form circular poles that are attached to full layers of particles. The dimensions of the gas channel remained the same but only the solid wall structure (target) is changed. The removed particles are compensated by the ghost particles in a way that the total number of particles of the structure remains the same regardless of the number and size of the poles. In the structure shown in figure 3 there are three rows of poles with three poles in each row for a total of nine poles. The first and

third rows are in line with each other and the second is offset by half the distance between any two rows. All the poles have the same diameter and depth. Porosity is controlled by varying the poles diameter. In all cases the depth is set to $9.66\psi_w$. The volume occupied by the poles particles is the cross sectional area multiplied by the poles length. The poles are attached to a solid wall (target) that has an axial length of $16.1\psi_w$.

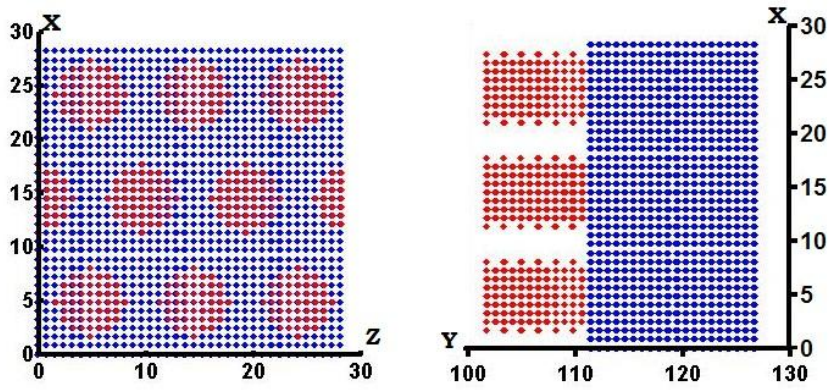

Figure 3: Schematic view of porous material structure with straight poles attached to solid structure.

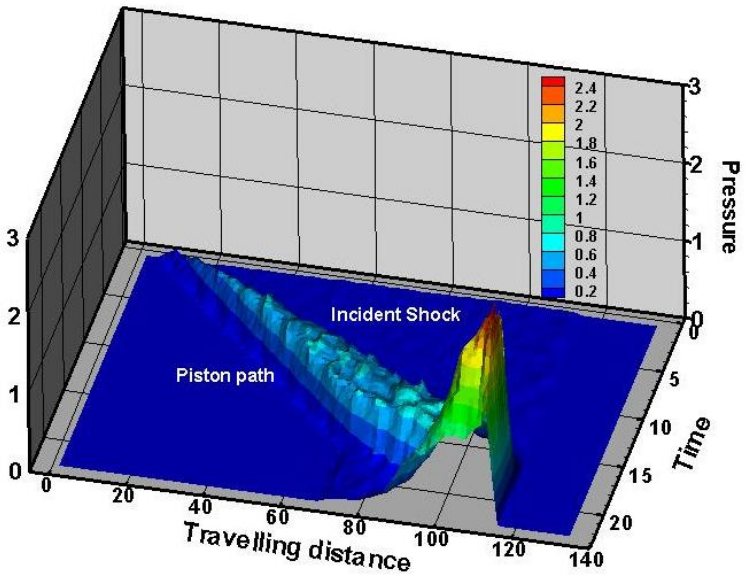

Figure 4.1: Pressure profiles in the gas channel with shock impacting a porous material structure with poles attached to end wall with 98% porosity. Length scale ψ_w, time scale $\psi_w(m_w/\phi_{0w})^{1/2}$,pressure scale ϕ_{0w}/ψ_w^3.

During the formation of the poles, a desired value of the pole diameter was set. However, porosity cannot be calculated based on this diameter since the position vector has discrete values and there always will be a deviation between the desired diameter value and actual size of the produced poles. Porosity was calculated based on the number of particles in the volume occupied

by the poles particles only divided by the number of solid and ghost particles in that volume, $\eta = N_{solid} \ (N_{solid} + N_{ghost})$.

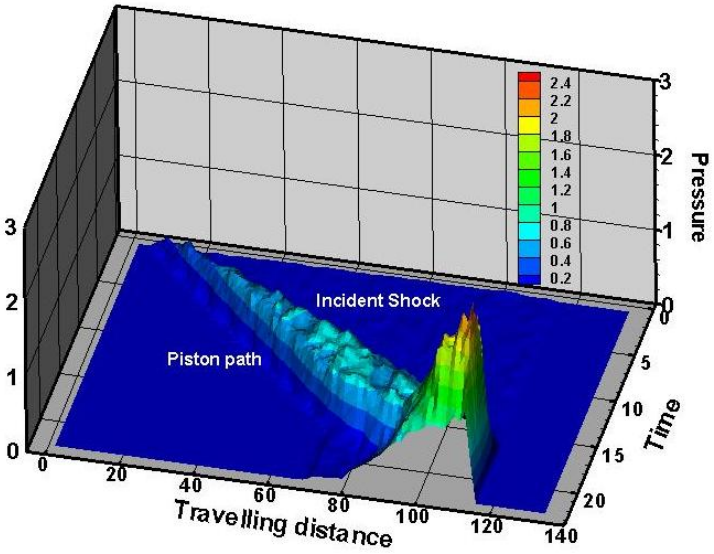

Figure 4.2: Pressure profiles in the gas channel with shock impacting a porous material structure with poles attached to end wall with 80% porosity.

Figures 4.1 & 4.2 show the pressure contours along the gas channel at various times. A shock wave was formed and developed as it was discussed earlier and it propagated in the gas channel till it reached the porous wall. At this location, part of the shock impacts the pole face and then reflected back towards the piston: this is the *primary reflection*, while the other part of the shock keeps propagating in the space between the poles, impacting the base of the wall and then reflected backwards in the opposite direction a process designated as *secondary reflection*. The results in figure 4.1 & 4.2 show that the secondary reflection results in higher pressure rise than the primary one at t=0.20. However, if a comparison to the data in figure 2.1 is made, one can conclude that in the case of porous wall, the pressure behind the reflected shock is always less than that of a solid wall. As porosity increases primary reflection strength weakens less and secondary reflection becomes stronger. The outcome of this split reflection depends on the frontal reflecting area ratio. For the same depth of each test case lower porosity is equivalent to higher frontal area associated with the primary reflection. On the other hand higher porosity results in higher reflecting area in the back wall.

Of interest is a comparison of these data to the corresponding data obtained in the case of a shock impacting a pure solid wall only without any porous front structure. This case is simply designated as a case with η=1.00 porosity. The change in energy of the solid structure associated with the transmitted stress is computed by calculating the work done by the strained structure and plotted in figure 5 for two cases of porosity. The results show that less energy is transmitted to the target wall when a porous structure is attached upfront. This reduction in transmitted energy depends on porosity and is higher in structures with lower porosity. In the present case of a porous wall with η=0.80, it is by 30% lower than that with η=1.00. This clearly demonstrates the advantage of porous structures in attenuating the energy of the impact. There is also a time

delay due to the presence of poles on the onset of energy transmission. Energy starts to build up earlier when the porosity is lower. In addition, the higher the porosity, the higher and steeper the transmitted energy during shock impact.

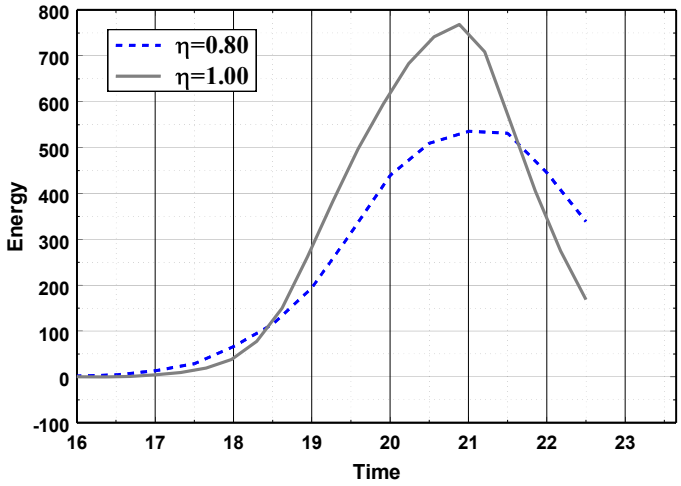

Figure 5: Variation of the change in energy of solid wall particles during shock impact.

CONCLUSIONS

The results indicate that the presence of nano-porous material layers in front of a target wall appears to have beneficiary effects on its survivability. First, it reduces the deposited energy by about 30% when compared to the non-protected target case which is equivalent to a fully porous material with 100 percent porosity. Second, it decreases the loading rate of the target wall and thus further protecting the integrity of the structure. Additional work is required to fully document the behavior of such materials during shock impact in different geometric arrangements, sizes, properties and parameters.

Acknowledgments The financial support provided by NSF under Grant CCI-0800307 is greatly appreciated.

REFERENCES

Allen, M.P., Tildesley, D.J. (1987). *Molecular Simulation of Liquids.* Oxford University Press, Oxford.

Al-Qananwah A. K., Koplik J., Andreopoulos, Y. (2013). "Shock Wave Interactions with Nano-structured Materials: a Molecular Dynamics Approach" *Shock Waves*, DOI 10.1007/s00193-012-0397-4, Vol. 23(1), pp. 69-80.

Andreopoulos, Y., Xanthos, S., Subramaniam, K. (207). "Moving shocks through metallic grids: their interaction and potential for blast wave mitigation." *Shock Waves*, vol. 16(6), pp. 455-466.

Andreopoulos Y. (2013). "Shock waves impacting composite material plates: the mutual interaction" *J. of Materials*, 65:185-202, DOI 10.1007/s11837-012-0506-y.

Baer M.R., Nunziato, N.W. (1986). "A Two-Phase Mixture Theory for the Deflagration-to-Detonation Transition in Reactive Granular Materials." *Int. J. Multiphase Flow* **12** 861-889.

Bear J., Bachmat, Y. (1990). "*Introduction to Modeling Transport Phenomena in Porous Media"* (Klumer, Dordrecht).

Biot, M.A. (1941). "General Theory of Three Dimensional Consolidation." *J. Appl. Phys*. **12,** 155-164.

Gong, M. W., Andreopoulos, Y. (2008). "Shock Wave Impact on Monolithic and Composite Material Plates: The Preferential Aeroelastic Response". *J. Sound and Vibration* 313, 171–194.

Gong M. W., Andreopoulos, Y. (2009). "Coupled fluid–structure solver: The case of shock wave impact on monolithic and composite material plates". *J. Computational Physics* 228, 4400-4434, doi:10.1016/j.jcp.2009.03.009.

Gubaidullin, A.A., Britan, A., Dudko, D.N. (2003). "Air shock wave interaction with an obstacle covered by porous material", *Shock Waves* 13, 41-48.

Hess S., Kroger M. (2001). "Thermophysical properties of gases, liquids and solids composed of particles interacting with a short-range attractive potential", *Phys. Rev. E* 64, 011201.

Hess S., Kroger M. (2002). "Elastic and Plastic Behavior of Model Solids", *TECHNISCHE MECHANIK,* Band 22, Heft 2.

Kazemi-Kamyab V., Subramaniam K., Andreopoulos Y. (2001). "Stress transmission in porous materials impacted by shock waves" *J. Appl. Phys*. 109(1), 013523; doi:10.1063/1.3517791.

Koplik J., Banavar, J.R. (1995). Continuum Deductions from Molecular Hydrodynamics. *Annual Rev. Fluid Mech.* **27**, 257-292 (1995).

Levy, A. Sorek, S., Ben-Dor, G., Bear, J. (1995). "Evolution of the balance equations in saturated thermoelastic porous media following abrupt simultaneous changes in pressure and Temperature" *Transport in Porous Media* **21,** 241-268.

Mazor, G., Ben-Dor, G., Igra, O., Sorek, S. (1994). "Shock Wave Interaction with Cellular Materials: I. Analytical Investigation and Governing Equations." *Shock Waves* **3,** 159-165.

Seitz M.W., Skews, B.W. (1996). "Shock Impact on Porous Plugs with a Fixed Gap between the Plug and a Wall", in B. Sturtevant, J. E. Shepherd, H. G. Hornung, eds., *Proceedings of the 20th International Symposium on Shock Waves* (World Scientific, Singapore).

Seitz, M.W., Skews, B.W. (2006). "Effect of compressible foam properties on pressure amplification during shock wave impact." *Shock Waves,* 15,177-197.

Stankovic I., Hess S., Kroger M. (2004). "Structural changes and viscoplastic behavior of a generic embedded-atom model metal in steady shear flow" *Phys. Rev.* E 69, 021509.

Subramaniam, K., Nian, W., Andreopoulos, Y. (2009). "Response of an Elastic Structure Subject to Air Shock Considering Fluid-Structure Interaction". *International J. of Impact Engineering* 36, pp. 965-974.